한국해양환경공학회지
Journal of the Korean Society
for Marine Environmental Engineering
Vol. 10, No. 1. pp. 53-58, February 2007

선형이론의 이중확산 유체의 적용

황 진 환
한국환경정책평가 · 연구원 기후변화연구실

Application of Linear Dynamics to Salt Finger Favorable Flows

Jin Hwan Hwang†
Associate Research Fellow, Climate Change Research Group, Korea Environment Institute, Seoul Eunpyung-Gu, Bul-gwang-Dong, 613-2, Korea

요 약

하구에서 오염물은 salt finger가 발생할수 있는 적당한 조건하에서 혼합과 수송이 일어날수 있다(Hwang and Rehmann, 2004). 선형이론을 salt finger가 일어날수 있는 적절한 조건하에 유체의 운동을 예측하는데 적용하였다. 모의 결과는 기존의 실험 결과와 거의 비슷한 결과를 도출하였다. 밀도율이 2보다 클 때, Turner(1967)가 열과 소금을 이용한 실험에서 발견한 것처럼 혼합율(the flux ratio)은 0.55~0.57를 보이며, 소금과 설탕을 이용한 Griffiths(1980)의 실험에서와 같이 0.87의 혼합율을 도출하였다. 두개의 매계 물질의 분자확산계수가 증가함으로써 이송속도율도 밀도율과 함께 증가하였고, 높은 밀도율에서 이송속도율이 정상상태가 되는데 걸리는 시간이 증가하였다.

Abstract – In an estuary, mixing and transport of contaminant sometimes occurs in the salt finger favorable condition (Hwang ang Rehmann, 2004). Linearized theory is applied to predict flow dynamics in salt finger favorable condition. The simulated results match well with previous laboratory experiments. When the density ratio is larger than 2, the heat and salt system shows 0.55~0.57 as Turner (1967) found, and the salt and sugar system produces 0.87 of Griffiths (1980). As the ratio of molecular diffusivities of two scalars increases, the flux ratio increases. The flux and eddy diffusivity ratios decrease with increase of density ratio, and it takes longer time for flux ratio to be steady state at the higher density ratios.

Keywords: Double-Diffsion(이중확산), Salt-finger(염분손가락), Turbulence(난류), Mixing(혼합), Estuary(하구), Saemangum(새만금)

1. INTRODUCTION

Salt fingering is one of the dominant processes of thermohaline mixing and transport in the ocean (Gregg, 1987). In the estuary, where warm salt sea water meets with cold fresh water from river, salt finger process can occur and change the mixing properties of salinity, heat and contaminants. Even though the exact contribution of double diffusion to mixing is not yet determined clearly nor studied well, this special processes are also observed in the estuarian mixing like as in Saemangum lake winter mixing (Hwang and Rehmann, 2004)}. Compared with small scale turbulence driven mixing, salt finger has much higher transport rates of heat and salt. Salt fingering also has higher salt flux than heat flux, which are assumed as equivalent to each other in the oceanic numerical models. The importance of different transport rates of heat and salt in the ocean models was emphasized by Gargett and Holloway (1992). In particular, the salt fingering contribution to circulation model was presented by Zhang *et al.* (1998).

Even though the salt fingering is an important process in thermohaline mixing, it is very complicated to find the transport properties in diverse systems through laboratory and numerical experiments, which were considered to study the physics of salt fingers (e.g., Turner (1967), Radko and Stern (1999)). To avoid heat loss or fast convection process,

†Corresponding author: jinhwang@kei.re.kr

laboratory experiments have been performed with salt-sugar system instead of heat-salt system (e.g., Krishnamutri (2003), Wells (2001b)). Laboratory experiments also have limitations on the boundary effects and sharp interface of heat and salt. Even though the direct numerical model simulation (DNS) is possible with higher Prandtle number (Pr) and smaller Lewis number(τ), it is hard to simulate long enough and expensive to capture the whole evolution of salt fingers until flux ratios reach certain critical state.

Schmitt (1979) solved linear equations based on linear stability analysis and found a relationship between the maximum growth rate and other parameters such as the density ratio R_ρ, Lewis number τ and Prandtl number Pr, when density ratio can be defined as

$$R_\rho = \frac{\alpha \Delta T}{\beta \Delta S} \tag{1}$$

The present work solves a set of linearized equations, which are similar to Schmitt (1979b), to overcome the limitations of the laboratory and direct numerical simulation studies. While Schmitt solved the problems based on the linear stability analysis, the present work derived equations from a linear turbulence equation and can include other directional momentum equations. Solving the linearized equations has advantages in using lower molecular diffusivity of salt, calculating faster than the whole set of non-linear turbulence equations and avoiding mathematical complexity of linear stability analysis.\par

2. METHODS

When the time scale of the mean flow is smaller than that of the turbulence in stably and unstably stratified flows, non-linear terms can be neglected. Hanazaki and Hunt (1996) applied linear dynamics to stably stratified flows, Townsend (1976) presented linear turbulence model results for Bénard convection, and Hanazaki (2002) also predicted flow behavior in a unstable flow. Comparing buoyancy terms with non-linear terms,

$$\frac{u^2}{l} / uN = \frac{u}{Nl} \ll 1 \quad .$$

When u is the velocity fluctuation scale, l is the length scale, and N is the buoyancy frequency, Hanazaki and Hunt (1996) showed that linear theory can be applied to predict turbulence based on the Froude number of $Fr = (u/Nl^2)^{1/2}$ and in the range of

$$Fr \ll 1 \tag{2}$$

We treat homogeneous turbulence in a fluid subject to linear temperature and salinity profiles. When the assumptions are applied to governing equations, nonlinear terms can be neglected. We introduce a Fourier representation of the dependent variables; for example,

$$u_j(\xi, \hat{t}) = \sum_{\underline{k}} \hat{u}_j(\underline{k}, t) e^{-ik_j \xi_j} \tag{3}$$

where k_j is the wave number in the j-direction, $i = \sqrt{-1}$, and the hats denote Fourier amplitudes. Salinity and temperature mean profiles are defined with each $(d\bar{S}/dx_3)^{1/2}$ and $(d\bar{T}/dx_3)^{1/2}$. Time scale is defined with $1/N$ and dimensionless time is $\hat{t} = Nt$. The temperature term is $\hat{u}_T(g\alpha T/N)$ and the salinity term $\hat{u}_S = g\beta S/N$ is when α is thermal expansion coefficient and β is haline coefficient. The Reynolds number, Re is Nl^2/ν. Then, when the pressure is eliminated with the continuity equation, the resulting system is

$$\frac{d\hat{u}_1}{d\hat{t}} = \frac{k_1 k_3}{k^2}(\hat{u}_S - \hat{u}_T) - \frac{1}{Re} k^2 \hat{u}_1 \tag{4}$$

$$\frac{d\hat{u}_2}{d\hat{t}} = \frac{k_2 k_3}{k^2}(\hat{u}_S - \hat{u}_T) - \frac{1}{Re} k^2 \hat{u}_2 \tag{5}$$

$$\frac{d\hat{u}_3}{d\hat{t}} = \left(\frac{k_3^2}{k^2} - 1\right)(\hat{u}_S - \hat{u}_T) - \frac{1}{Re} k^2 \hat{u}_3 \tag{6}$$

$$\frac{d\hat{u}_T}{d\hat{t}} = \frac{N_T^2}{N^2}\hat{u}_3 - \frac{1}{Re \cdot Sc_T} k^2 \hat{u}_T \tag{7}$$

$$\frac{d\hat{u}_S}{d\hat{t}} = \frac{N_S^2}{N^2}\hat{u}_3 - \frac{1}{Re \cdot Sc_S} k^2 \hat{u}_S \tag{8}$$

when $N_T = g\alpha(d\bar{T}/dx_3^2)^{1/2}$ and $N_S = g\beta(d\bar{S}/dx_3^2)^{1/2}$ are the temperature and salinity mean fluctuating frequencies and the buoyancy frequency can be defined by $N^2 = N_T^2 - N_S^2$. When transport equations are derived from the above fluctuation equations, then the vertical scalar flux or correlation term can be defined as

$$\frac{\partial E_{3T}}{\partial t} = \left(\frac{k_3^2}{k^2} - 1\right)(E_{TS} - E_{TT}) + \frac{N_T^2}{N^2} E_{33} - \frac{N_T^2}{Re}\left(1 + \frac{1}{Sc_T}\right) E_{3T} \tag{9}$$

The more detailed derivation of each terms are defined in Rehmann and Hwang (2004). The given correlation equations become a set of ordinary differential equations and solved by the stiff method using LSODA package.

3. RESULTS

Fig. 1 presents the flux ratios depending on the Lewis numbers. When turbulence mixes two scalars, the flux ratio

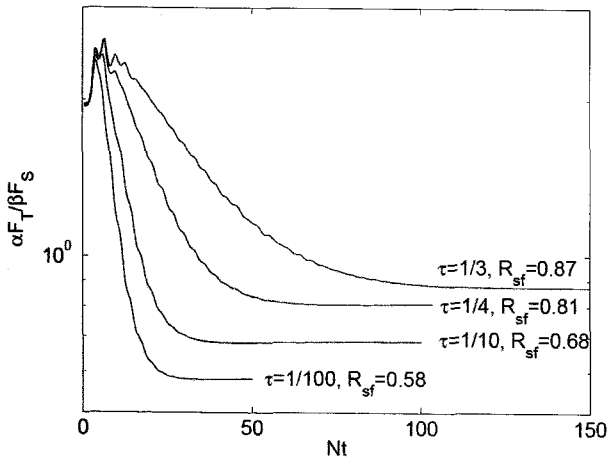

Fig. 1. Flux ratios for various Lewis numbers. When τ is 1/100 (heat and salt), flux ratio is 0.58, which is similar to Turner (1967) and when τ is 1/3 (salt and sugar), flux ratio is 0.87, which was observed by Griffiths (1980) in laboratory experiment.

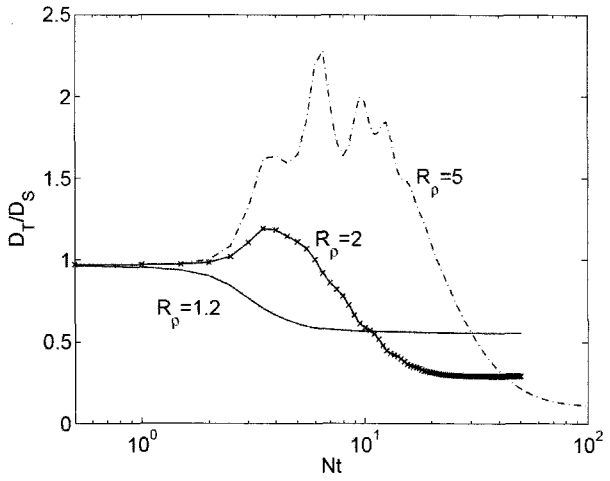

Fig. 2. Diffusivity ratio as a function of density ratio. The numbers under the line indicates the density ratios.

will equal the density ratio when the eddy diffusivities of salt and heat equal. After initial turbulence kinetic energy is damped by stratification, salt fingers control the mixing. In that case, the density ratio no longer equals the flux ratio.

The present simulation produces flux ratio similar to those observed in previous laboratory experiments. When τ is 1/100 corresponding to a heat and salt system and R_ρ is larger than 2, the flux ratio is 0.58, which was similar to 0.56 of Turner's experiment. Griffiths (1980) found 0.88 in the salt-sugar laboratory experiment, when density ratio is larger than 2. The present work used a Prandtl number of 7 to model the stably distributed scalar instead of 700 of salt and a Prandtl number of 21 for the unstably distributed scalar instead of 2100 for sugar to reduce computing time and remove numerical instability. However, the present results produce a flux ratio of 0.87, which is similar to that in Griffiths (1980). As Schmitt (1983) described, the Prandtl number is not critical in the case of the large Lewis number. For all Lewis numbers, the flux ratios follow similar evolution. When τ is 1/100, the flux ratio deviates from other cases, and decreases toward 0.58. As the Lewis number increases, the maximum value of the flux ratio appears later and approach a larger final value.

Fig. 2 presents the eddy diffusivity ratios as a function of time for various density ratios. At the initial time, the eddy diffusivity ratio is smaller than 1 in all cases. At the lowest density ratio (R_ρ=1.2), the diffusivity ratio remains smaller than 1 until initial fluctuations are damped by the stratification. After initial fluctuations activate motion, the flux behavior is similar to the stably stratified flow. In this period, effects of salt fingers are negligible, and fluxes of salt and heat oscillate as in the strongly stratified flow. As time increases, the diffusivity ratio increases with higher density ratios. When the density ratio is 5, the diffusivity ratio grows over 2, and after fluctuations are damped and salt fingers becomes dominant, the diffusivity ratio drops to 0.12, which is close to 0.1, the square root of the Lewis number. The steady state of diffusivity ratio appears at the later time as density ratio increases.

In the earlier period of Fig. 2 $Nt<1$, diffusivity ratio is slightly smaller than 1. Before simulation, we expected that this may be exact 1, however, the simulation produced the different results from our expectation. Hanazaki and Hund (1996) showed that the linear theory can explain turbulent flows in a very short period and linear theory can be applied independently from whether flow is stratified or not. The derivation of each transport equation is similar to Hanazaki and Hunt (1996). After the fourier transforming, the equations are expanded by the power series or perturbation method in a short period such as

$$E_{33} = E_0 + \tau E'_{33} + \tau^2 E''_{33} + O(\tau^3) \quad (10)$$

$$E_{3T} = E_{3T}(0) + \tau E'_{3T} + \tau^2 E''_{3T} + O(\tau^3) \quad (11)$$

$$E_{TT} = E_{TT}(0) + \tau E'_{TT} + \tau^2 E''_{TT} + O(\tau^3) \quad (12)$$

$$E_{ST} = E_{ST}(0) + \tau E'_{ST} + \tau^2 E''_{ST} + O(\tau^3) \quad (13)$$

After putting the above terms into transport equations, each coefficients can be derived by ignoring the higher order terms and the results are integrated through volume in the

spherical coordinate. After the integration of θ and ϕ is numerated, heat and salt transport equations become

$$\alpha E_{3T} = \alpha \overline{wT} = \alpha N_T^2 \pi \int_k (4 - 6Re^{-1}k^2\tau - 2Re^{-2}Sc_T^{-1}k^2\tau)\tau E_0(k)dk \quad (14)$$

$$\beta E_{3S} = \beta \overline{wS} = \beta N_S^2 \pi \int_k (4 - 6Re^{-1}k^2\tau - 2Re^{-2}Sc_S^{-1}k^2\tau)\tau E_0(k)dk \quad (15)$$

when α and β are heat and salt expansion coefficient and N_T^2 and N_S^2 are the gradients of heat and salt. The density ratio R_ρ can be defined as $\alpha N_T^2/\beta N_S^2$ that is assumed simply to be 1. Based on the above relationships, the eddy diffusivity ratio of heat and salt is defined as

$$\frac{D_T}{D_S} = \frac{\int_k (2 - 3Re^{-1}k^2\tau - Re^{-1}Sc_T^{-1}k_2)E_0(k)dk}{\int_k (2 - 3Re^{-1}k^2\tau - Re^{-1}Sc_S^{-1}k_2)E_0(k)dk} \quad (16)$$

The eddy diffusivity ratio is smaller than 1, since Sc_S is larger than Sc_T. Therefore, the eddy diffusivity of salt with smaller molecular diffusivity is larger than that of heat. As the Reynolds number decreases, the diffusivity ratio decreases to smaller magnitude (Fig. 3). This indicates that as turbulence becomes stronger, the diffusivity ratio increases and becomes closer to 1. If turbulence is not strong enough, however, then salt flux is larger than heat flux. Amplitudes of fluctuations have sinusoidal forms (Hanazaki and Hunt, 1996) and this implies oscillation or rotation. As amplitude of velocity increases, the flux of heat increases faster than that of salt.

The flux coefficients are compared with the previous results from the linear theory and laboratory experiment

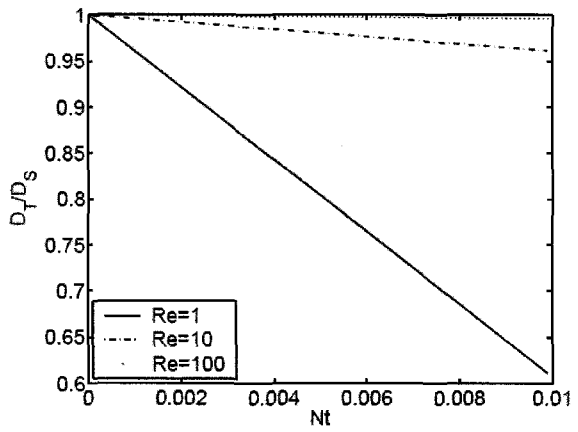

Fig. 3. Eddy diffusivity ratio in the different turulence Reynolds number of $\varepsilon/\nu N^2$.

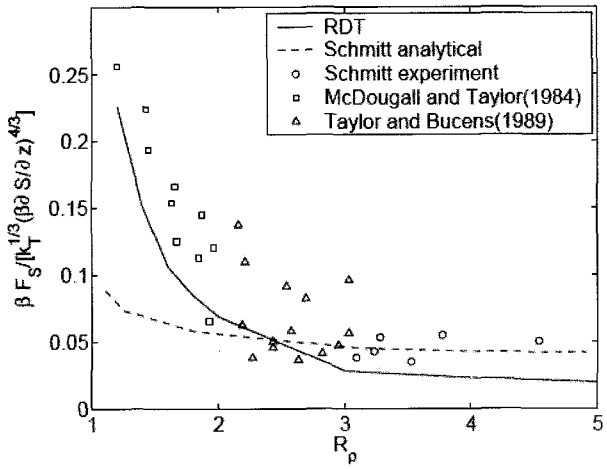

Fig. 4. The comparison of the flux coefficient with the previous works. τ is 0.01, and Re=10 for the present case. Solid line shows the present work, dotted line indicates Schmitt (2003), round markers present Schimtt (1979a), square maekres show McDougal and Taylor (1984) and triangle does Taylor and Buens (1989).

(Fig. 4). The flux is determined when the flux ratio becomes an asymptotic value. Kunze (2003) compared flux coefficients of the previous results. The flux coefficient of salinity is defined as

$$C_S = \frac{\beta F_S}{k_T^{1/3}(\beta\partial\bar{S}/\partial z)^{4/3}} \quad (17)$$

The exponent of the gradient in the denominator is not universal. Turner (1967) suggested 4/3, which is used in the present work and Kelley (1990) showed 5/4. Taylor and Veronis (1996) also found that 4/3 is not universal. Even though the previous works propose different power law, we choose an exponent of 4/3 to make the problem simpler for comparison.

Linear theory predicts the flux coefficients well when the density ratio is smaller than 2. Beyond this density ratio, Schmitt's (1979) results match well with the previous works. While Schimtt found the flux of the fastest growing fingers, the present study derived the total flux instead of the flux of the fastest fluctuation at a wave number. When density ratio is small then the blob has larger bandwidth comparing the higher density ratio at which the blob is thinner. Therefore, when we integrate flux over whole scales, the present results match better than Schimtt's. When density ratio is larger than 3, the present results underestimate the flux coefficeint and Schmitt's results matches well to the previous laboratory experiment.

The experimental results produce the fluctuations of salinity

at each wave number with time. At each wave number, we found temporal minimum fluctuation S_1 and time of salinity (t_1) and after that time, fluctuation grows monotonically. At the final simulation time (t_2), the maximum fluctuation is determined as S_2. During period between t_1 and t_2, we found the growth rate. The growth rate can be calculated as

$$S_2 = S_1 \exp(G_N(k)(t_2 - t_1)) \tag{18}$$

$$G_N(k) = \frac{1}{t_2 - t_1} \log\left(\frac{S_2}{S_1}\right) \tag{19}$$

The maximum growth rate is determined at the maximum $G_N(k)$. The maximum growth rate wave number is normalized and transformed in the same way as Schmitt (1983). When the growth rate is expressed as G_N, the transformed growth rate (G) is $G_N(1 - R_\rho^{-1})^{1/2}/2\pi$.

From the maximum growth rate and scale analysis of salt fingers, the bandwidth relationship can be defined. The scale of salt fingers has been investigated in previous work. Stern's (1975) analysis suggests that the salt finger wavelength is

$$\lambda_T = \left[\frac{g\left(\alpha\frac{\partial T}{\partial z}\right)}{\nu k_T}\right]^{\frac{1}{4}} \tag{20}$$

Other possible length scales are

$$\lambda_\rho = \left[\frac{g\left(\alpha\frac{\partial T}{\partial z}\right) - g\left(\beta\frac{\partial S}{\partial z}\right)}{\nu k_T}\right]^{\frac{1}{4}} \tag{21}$$

and

$$\lambda_S = \left[\frac{g\left(\beta\frac{\partial S}{\partial z}\right)}{\nu k_S}\right]^{\frac{1}{4}} \tag{22}$$

Tritton (1988) derived

$$\left[\frac{\delta}{L}\right]^4 \approx \frac{1}{Re_S} \tag{23}$$

where δ is the wavelength of salt fingers and L is the layer thickness. If we rewrite Tritton's relationship as the present expression, then salinity length scale becomes equal to equation (22).

The wavenumber ratio for bandwidth is derived with equations (21) and (22). One can define the marginal stable wave number as k_{min}, which is the inverse of λ_ρ and the marginal unstable wavenumber as k_{max}, which is the inverse λ_S. From the two marginal wavenumbers, the bandwidth

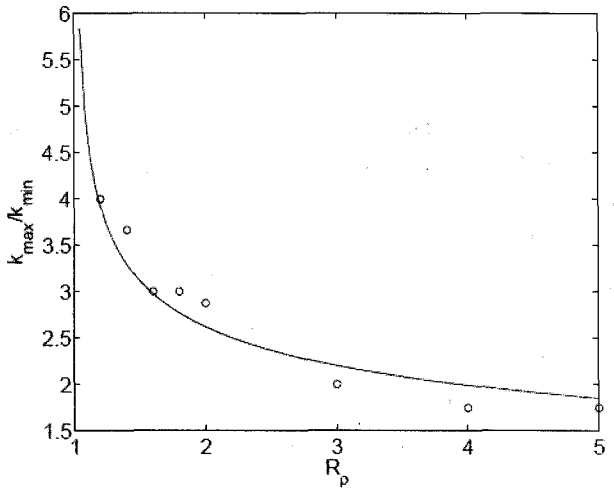

Fig. 5. Dependence of the bandwidth at Re=10 on R_ρ.

relationship can be defined as

$$R_\lambda = C\frac{k_{max}}{k_{min}} = C\left[\frac{\lambda_S}{\lambda_\rho}\right]^{-1} = C\left[\frac{\alpha\frac{\partial T}{\partial z} - \beta\frac{\partial S}{\partial z}\frac{k_S}{k_T}}{\beta\frac{\partial S}{\partial z}}\right]^{\frac{1}{4}}$$

$$= C((R_\rho - 1)\tau)^{-\frac{1}{4}} \tag{24}$$

where C is the bandwidth coefficient. As density ratio decreases, the bandwidth increases. The bandwidth of salt fingers also depend on the Lewis number. As the Lewis number becomes smaller, the bandwidth of salt finger becomes larger. Therefore, a salt-sugar system ($\tau \approx 1/3$) has a smaller bandwidth than a heat-salt system ($\tau \approx 1/100\tau$). Schmitt (1983) defined the bandwidths of wavenumbers, which have the growth rates satisfying $\exp(2\lambda/\lambda_m) = 1/e^2$, where λ_m means the maximum growth rate. We determined the bandwidth based on Schmitt's e-folding time definition of growth rate, $t = 1/\lambda_m$. Two wave numbers satisfying this relationship are k_{min} and k_{max}, which have the growth rates equivalent to 0.653 times of the maximum growth rate.

Fig. 5 compares the results of the simulation and the equation 24. From the simulation results, we can get the bandwidth coefficient which is 1.2 when the Lewis number is 0.01 corresponding to salt and heat. Fig. 5 presents the density ratio effects on the bandwidth. The simulation results show that the bandwidth is the function of 1/4 power of the density ratio as in equation 24. As density ratio increases, the bandwidth decreases. Since k_{max} is always larger than k_{min}, the bandwidth ratio decreasing means thinner shape of fingering growth. As density ratio decreases, the bandwidth ratio increases and the blob has more flatten shape.

4. CONCLUSION

Linearized theory is applied to predict dynamics of a flow in a salt finger favorable condition. When buoyancy controls the flow, nonlinear terms can be neglected by comparing the time scales. In particular, the time scale ratio ($\varepsilon/\nu N^2 \sim O(1)$) of salt fingers measured in the field was small enough to satisfy the assumption of linearized theory. In unsheared condition, the flux ratios of Turner (1967) and Lambert and Demenkov (1972)'s laboratory experiments are reproduced by the linearized simulation. When the density ratio is larger than 2, the heat and salt system shows 0.55$-$0.57 as Turner (1967) found, and the salt and sugar system produces 0.87 of Griffiths (1980). The Lewis number, the ratio of molecular diffusivities of stably and unstably stratified scalars, also determines the flux ratio which increases as the Lewis number increases. At a fixed Lewis number, the ratio of fluxes or eddy diffusivities of salt and temperature depend on the density ratio. As the density ratio increases, flux of eddy diffusivity ratios decrease, and it takes longer time for flux ratio to be steady state. When the maximum salt finger growth rate depends on the density ratio as predicted by Schmitt (1979), the relationship between the bandwidth is a function of the density ratio and the Lewis number.

REFERENCE

[1] Gargett, A. and Holloway, G., 1992, Sensitivity of the gfdl ocean model to different diffusivities for heat and salt. *J. Phys. Oceanogr.*, 22, 1158-1177.

[2] Gregg, M. and Sanford, T., 1987, Shear and turbulence in a thermohaline staircase. *Deep-Sea Res.*, 34, 1689-1696.

[3] Griffiths, R. and Ruddick, B., 1980, Accurate fluxes across a salt sugar finger interface deduced from direct density measurements. *J. Fluid Mech.*, 99, 85-95.

[4] Hanazaki, H., 2002, Linear processes in stably and unstably stratified rotating turbulence. *J. Fluid Mech.*, 465, 157-190.

[5] Hanazaki, H. and Hunt, J., 1996, Linear processes in unsteady stably stratified turbulence. *J. Fluid Mech.*, 318, 303-337.

[6] Hwang, J. and Rehmann, C., 2005, The shear effects on the salt finger favorable interface. *Proceedings of IAHR 2005*, IAHR, 4233-4240.

[7] Kelley, D., 1990, Fluxes through diffusive staircases: A new formulation. *J. Geophys. Res.*, 95, 3,365-3,371.

[8] Krishnamurti, R., 2003, Double-diffusive transport in laboratory thermohaline staircases. *J. Fluid Mech.*, 483, 287-314.

[9] Kunze, E., 2003, A review of oceanic salt-finger theory. Prog. Oceanogr., 56, 399-417.

[10] Lambert, R. and Demenkow, J., 1972, On vertical transport due to Øngers in double diffusive convection. *J. Fluid Mech.*, 54, 627-640.

[11] McDougall, T. and Taylor, J., 1984, Flux measurements across a finger interface at low values of the stability ratio. *J. Mar. Res.*, 2, 1-14.

[12] Radko, T. and Stern, M., 1999, Salt fingers in three dimensions. *J. Mar. Res.*, 57, 471-502.

[13] Rehmann, C. and Hwang, J., 2005, Small-scale structure of strongly stratified turbulence. *J. Phys. Oceanogr.*, 35, 151-164.

[14] Schmitt, R., 1979a, Flux measurements in an interface. *J. Mar. Science*, 37, 419-436.

[15] Schmitt, R., 1979b, The growth rate of super-critical salt fingers. Deep-Sea Res., 26A, 23-24.

[16] Schmitt, R., 1983, The characteristics of salt finger in a variety of fluid systems, including stellar interiors, liquid metals, oceans, and magmas. *Phys. Fluids*, 26, 2373-2377.

[17] Stern, E., 1975, Ocean Circulation Physics, *volume 19 of International Geophysics Series*. Academic Press.

[18] Taylor, J. and Bucens, P., 1989, Laboratory experiments on the structure of salt fingers. *Deep-Sea Res.*, 36, 1675-1704.

[19] Taylor, J. and Veronis, G., 1996, Experiment of double-diffusive sugar-salt fingers at high stability ratio. *J. Fluid Mech.*, 321, 315-333.

[20] Townsend, A., 1976, *The Structure of Turbulent Shear Flow*. Cambridge, U.K., 2nd edition.

[21] Tritton, D., 1988, *Physical Fluid Dynamics*. Oxford Science Publications, Oxford, U.K.

[22] Turner, J., 1967, Salt fingers across a density interface. *Deep-Sea Res.*, 14, 599-611.

[22] Wells, M., 2001b, *Convection, turbulence mixing and salt fingers*. Ph: D: thesis, The Australian National Univeristy.

[23] Zhang, J., Schmitt, R. and Huang, R., 1998, Sensitivity of GFDL modular ocean model to the parameterization of double-diffusive process. *J. Phys. Oceanogr.*, 28. 589-605.

2006년 8월 28일 원고접수
2007년 1월 3일 수정본 채택